DEVELOPMENT OF HIGH Nb CONTAINING HIGH TEMPERATURE TiAl ALLOYS

Guoliang Chen[1], Junpin Lin, Xiping Song, Yanli Wang, and Yunrong Ren
State Key Lab. for Advanced Metals and Materials
University of Science and Technology Beijing,
Beijing, 100083, China

Abstract

γ-TiAl alloy have been developed into two categories: conventional TiAl and high temperature TiAl (High Niobium containing) alloys. These state-of-the-art alloys have great advantage that the service temperature is 60-100 °C higher than that for conventional TiAl alloy. The relations between composition, microstructure and properties for high temperature TiAl alloys have been shown in the paper, including the quasi-binary phase diagram with high Nb contents, the high temperature strengthening mechanisms of Nb, Al and other elements, microstructure stability and degradation at high temperature, the creep property improvement and its relations with microstructure parameters. The paper also indicates further development of high temperature TiAl alloys.

Introduction

TiAl alloys have received considerable attention due to their attractive properties such as low density, excellent specific strength and good oxidation resistance. However, the conventional TiAl alloys are not strong enough for a wide range of applications especially at temperatures higher than 760-800°C. The high temperature strength of TiAl alloys strongly depends on the strain rate due to thermally activated glide and climb of dislocations as well as twining [1,2]. The potential for a significant increase of the high temperature strength merely through microstructural modification seems to be limited. We found that Nb is an essential additive in gamma TiAl alloys from the standpoint of oxidation resistance [3]. On the other hand, Nb element is highly soluble in the TiAl alloy so that it can be added in substantial volume [4-5]. High Nb-containing TiAl alloys developed by Chen et al. [6-14] were suggested to be the first example for the development of high temperature high performance TiAl alloys by Dr. Young-Won Kim in the First International Symposium on Gamma TiAl in 1995 [15]. Chen's group cooperated with Appel, Kim, Loretto etc. [16-22] has made a great effort to develop the high temperature TiAl alloy in recent years. Great progress has been made in the research, processing and application of high Nb-containing TiAl alloy. TiAl alloy have been developed into two categories: conventional TiAl and high temperature TiAl (high Niobium containing) alloys. The basic characteristics of high temperature TiAl alloys (high Niobium containing) can be described as:

(1) The service temperature is 60-100 °C higher than that of conventional TiAl alloy. The room temperature strength is ~300-500 MPa higher than that of conventional TiAl alloy. The mechanical properties are comparable to the conventional Ni base superalloys for disc application while the density is about half of the superalloys. The oxidation resistance is higher than that of conventional TiAl alloys, and similar to the excellent Ni-based superalloys.

(2) The basic compositional characteristics of the high temperature TiAl alloys are high Nb and low Al content, typically 6/9 Nb and 45-46Al. Carefully microalloying using the elements C, B, Si, W, Mn and rare earth elements may further optimize the properties of the alloys.

(3) Full lamellar structure with the grain boundaries having serrated morphologies is the basic microstructure. Stable B2 phase must be avoided. The important aspect is to optimize the microstructure with a target of the homogeneous α fine lamella with straight lamellar boundaries distributed in fine grains.

The present paper briefly introduce the relations between composition, microstructure and properties of the high-Nb containing TiAl alloys, including the quasi-binary phase diagram with high Nb contents, the high temperature strengthening mechanisms of Nb, Al and microalloying, microstructure stability and degradation at high temperature, creep property improvement and its relations with microstructure parameters. The possible application as well as further development in raising service temperature is discussed.

Effect of Nb addition in the phase transformation of TiAl alloy

The quasi-phase diagrams of Ti-(44-49)Al with 8Nb and 10Nb (at. %) addition (solid lines) is shown in Fig. 1 [12]. The binary Ti-Al phase diagram is presented as dotted lines in the figure for comparison. It can be seen that 8-10 Nb addition has pronounced effect on the phase relationship of γ-TiAl alloys. The effects are summarized as follows.

(1) The melting point (solidus) increases by about 100 ^{o}C, for example, from ~1500 of Ti-45Al alloy to 1610 ^{o}C of Ti-45Al-10Nb alloy. Raising melting point is the most important consideration of the alloy design for high temperature application.

(2) The β(B2) transus ($\beta/\alpha+\beta$ boundary) decreases by 50-80 ^{o}C, and the β(B2) phase region is extended to higher Al concentration.

(3) The α transus decreases by about 30 ^{o}C. The $\alpha/\alpha+\beta$ transus decreases by 50-100 ^{o}C. The α phase region is narrowed and moved to higher Al concentration.

(4) The γ phase region is extended to lower Al concentration. For example, the Al content of γ phase at 1050 ^{o}C decreases from 48 Al for Ti-45Al to 45.5 Al for Ti-45Al-10Nb alloy. This point is favorable to the room ductility of the alloy.

(5) The $\alpha \rightarrow \alpha_2+\gamma$ eutectoid temperature appears to increase to ~1170 ^{o}C for 8 Nb addition.

(6) The low temperature phase region ($\alpha_2+\gamma$) is replaced by the $\alpha_2+\gamma$+B2 ternary phase region when Nb content exceeds 9.5%. This point restricts the upper limit of Nb content in the alloy because the harmful B2 phase must be avoided.
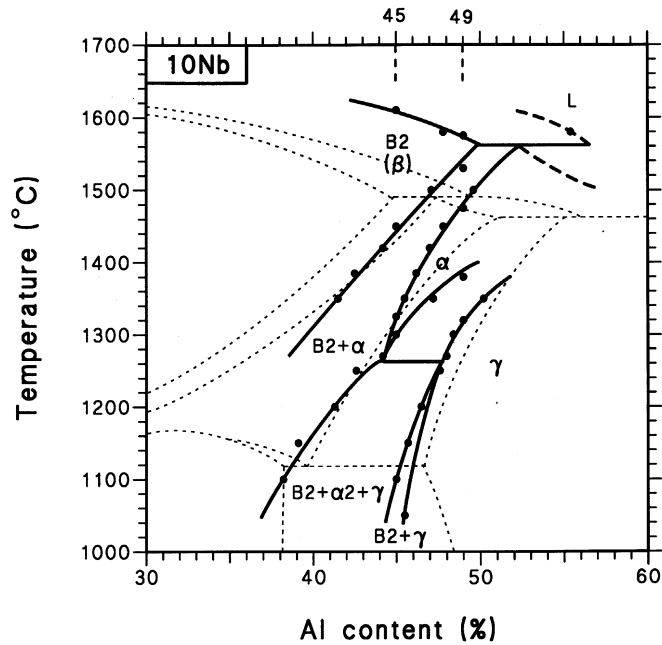
Fig. 1 Quasi-phase diagrams showing the effect of 8Nb and 10 Nb additions on the phase relationship of near γ-TiAl alloys (solid lines). The binary Ti-Al diagram is drawn in dotted lines for reference.

Alloy chemistry, microstructures and tensile properties of high temperature TiAl alloy

A class of high temperature TiAl alloys has been designed. The compositions of these alloys range:
Ti-(45-46)Al-(6-9)Nb-x(W, Mn, Hf)-y(C, B)-z(Y, Rare earth).

As shown, the basic compositional characteristics of the high temperature TiAl alloys are high Nb and low Al content, typically 6/9 Nb and 45-46Al. Carefully microalloying using C, B, Si, W, Mn and rare earth elements may further optimize the properties of the alloys. Refractory elements W, Hf and C can effectively enhance high temperature strength and creep resistance by solid strengthening (W, Hf) or precipitate strengthening (C). The distribution of W in high Nb containing TiAl alloys is uniform. B is useful for grain refining and segregation of casting by precipitate of borides. Small amount of rare earth elements such as Y and Gd introduce more stable oxide layer that can improve oxidation resistance to the temperature as high as 900 $^{\circ}$C. Fig. 2 shows the effects of microalloying on the mechanical properties. C addition effectively increases tensile strength due to precipitate of Ti_3AlC particles. The orientation relationship between Ti_3AlC carbide and γ phase is
$$[100]_C//[100]_\gamma; \quad [001]_C//[001]_\gamma$$

Similar to the conventional TiAl alloys, four typical microstructures, i.e. fully lamellar (FL), nearly lamellar (NL), near-gamma (NG) and duplex (DP), of high temperature TiAl alloys can be obtained by heat treatments. The mechanical properties of four microstructures are shown in Fig. 3. The yield strengths of the Ti－45Al－10Nb alloys are much higher than those of conventional TiAl alloys. Fine grain NG alloy exhibits higher strength at room temperature, but reverse at high temperature. The critical issue in microstructural optimization is avoidance of stable B2 phase. Optimization of the alloy composition and processing may strongly control the segregation and the B2 phase. Fig. 4 indicates the harmful effects of B2 phase: enhancing cracking by its brittleness at room temperature and reducing high temperature strength by its quickly softening.
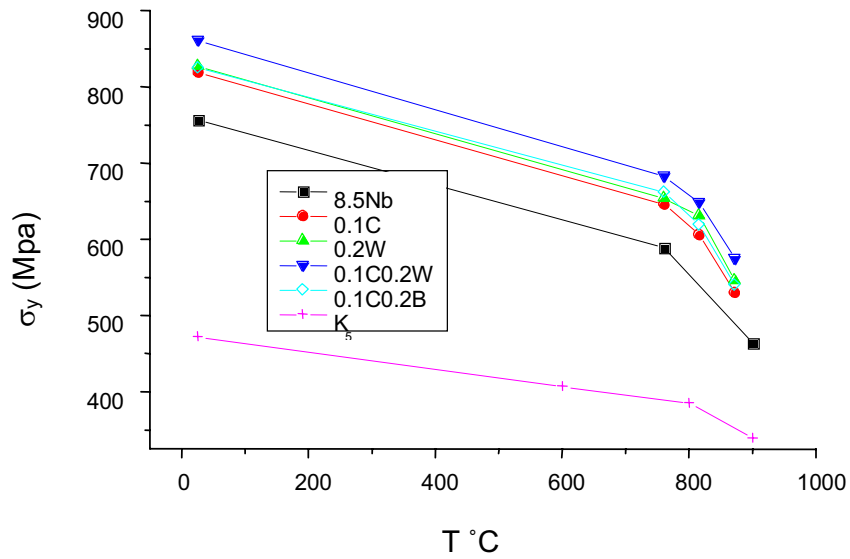
Fig.2　Effects of microalloying on the mechanical properties of high temperature TiAl alloys (FL microstructure, Lamellar spacing: 0.24-0.26 μm, Grain size: 160-190 μm)
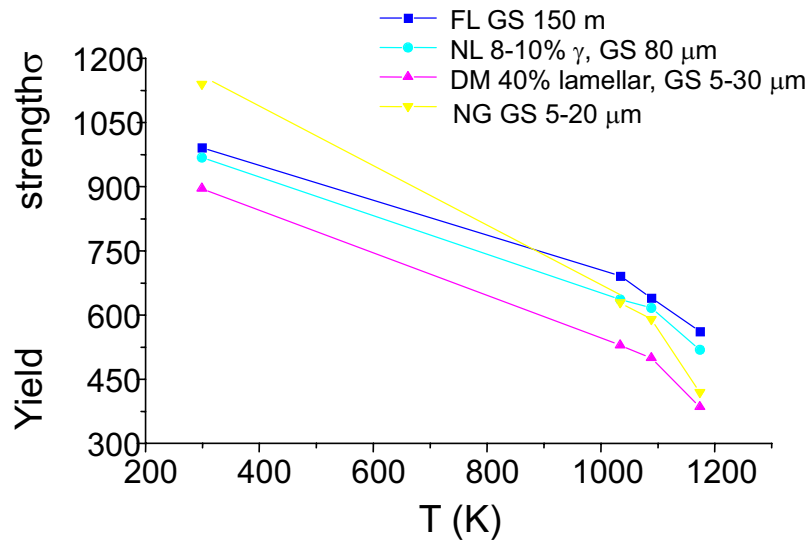

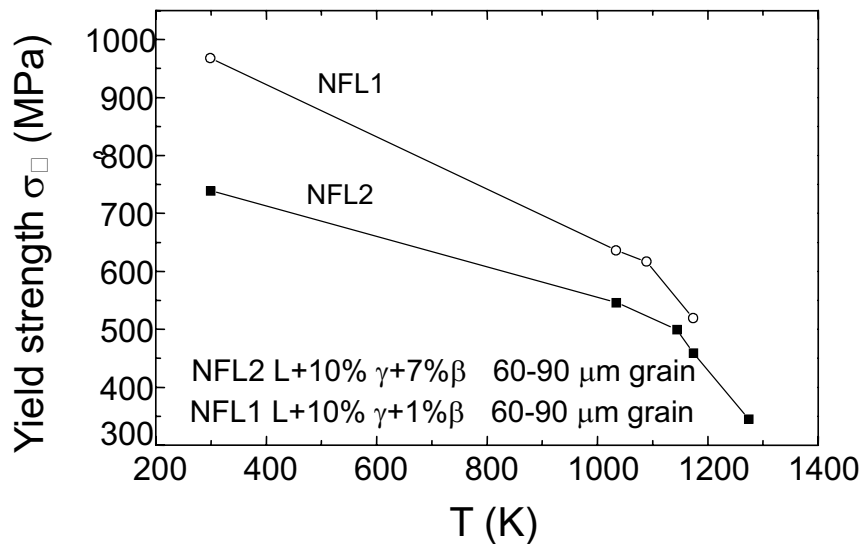Fig. 3　Tensile yield strengths of Ti-45Al-10Nb alloys with four typical microstructures

Fig. 4   Harmful effects of B2 phase in Ti-45Al-10Nb alloy

Strengthening mechanism of high temperature TiAl alloy

The experimental results illustrate that the high strength of high temperature TiAl alloy comes from the solid solution strengthening of high Nb additions. In contrast, Paul et al. [17] believed that the strengthening was simply due to the low Al content of the alloys and the related structural changes. They found that the Al content of the alloy had a greater influence than the niobium content. However, the authors noted that the materials used in their study had different microstructures. The lower Al containing alloys (Ti–45Al and Ti–45Al–10Nb) had a fully-lamellar microstructure with very fine lamellar spacing (0.1 μm), whereas, the higher Al containing alloys (Ti–49Al and Ti–48Al–10Nb) had a duplex or near gamma microstructure. Therefore, the strengthening effect of Nb and Al may be masked by the differences in microstructure. It is necessary to compare the strengths of different alloys in a form of similar microstructure. In addition, we should pay more attention to the high temperature strength.

Nb solution hardening for NG microstructure

The solid solution strengthening effect of Nb is clearly illustrated by Fig. 5. High Nb addition in NG significantly increases the high temperature strength. The differences in σ_y between ternary and binary alloys with same Al content are 85-150 MPa depending on Al content. The effect of Al in binary alloys on high temperature strength is slight (10 MPa). Low Al content may increase the amount of α_2 phase that may influence on the strength of alloys. Nevertheless, the differences in σ_y between ternary and binary alloys with same volume of α_2 phase are also significant as in the range of 96-170 MPa depending on the volume of α_2 phase. The solid solution strengthening of Nb at high temperature originates obviously from two sides: friction stress and diffusion related resistance of dislocation movement. The friction stresses (σ_0) were calculated by using the Hall–Petch equation, $\sigma_y=\sigma_0+kd^{-1/2}$, where σ_y is the RT yield strength, k the Hall–Petch constant (taken the value as 1 MPa m1/2) and d is the grain size [13]. The calculated friction stress of Ti-45Al-10Nb

is nearly 500 MPa higher than that of NG binary Ti-50Al and Ti-47Al-2Cr-0.2Si alloys.
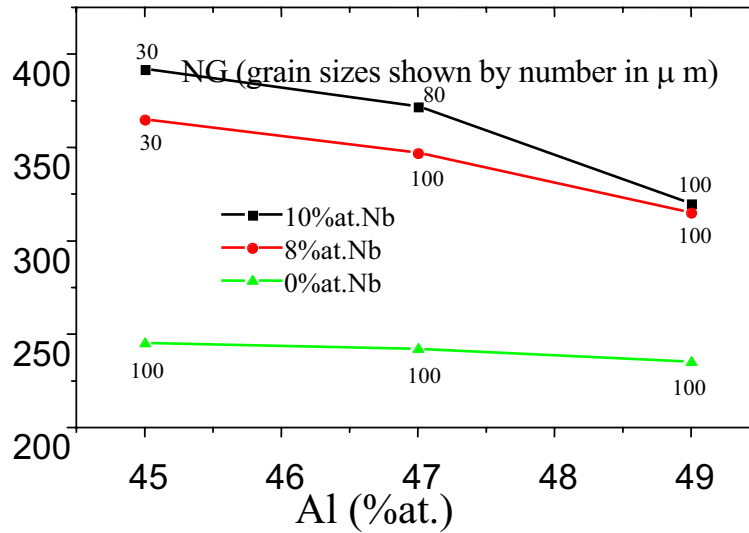

Fig. 5　Effects of Nb and Al on the 900 °C yield strength of high temperature TiAl alloys with NG microstructure

Because no precipitates were observed in the alloy by TEM observation, the high friction stress of NG Ti-45Al-10Nb alloy appears to originate from the solid solution hardening of high Nb additions. The detailed study [13] indicated that strong solid solution strengthening is expected due to the formation of Nb/Al anti-site defects because the size misfit for Nb on the Al sublattice was calculated to be very high, much higher than that for Ti on the Al sublattice. Although the Ti sublattice is the preferred site for Nb in the γ phase, the occupancy of Nb on the Al sublattice in Al-lean alloys is still feasible, especially in the alloys with lower Al concentration. The study of thermal activation approach [23] further indicates that the solid solution strengthening of Nb can be attributed to the increase of the thermal resisting stress τ^* and the athermal long-range elastic interaction with dislocation forest inside γ grain τ_{disl}. The value of τ^* and τ_{disl} are 117 MPa and 66 MPa while the data for conventional TiAl are 25 MPa and 10 MPa respectively.

Strengthening effect of Nb in FL microstructure

In order to examine whether the high strengths come merely from the strengthening of lamellar interfaces, the strengths of binary (-0 Nb) and ternary alloy (-10 Nb) were plotted as a function of the lamellar spacing for the alloys containing 44~49 at.% Al. Fig. 6 illustrates that the hardening effect of lamellar spacing at 900°C follows the Hall-Petch relation. The values of hardening coefficients k_λ for the alloys with Nb and without Nb additions are 0.14 and 0.12 MPa $\sqrt{m}$, respectively. These results suggested that the strengthening effect of lamellar interfaces is eventually the same in both binary TiAl and ternary TiAl-10Nb alloys. The value of k_λ observed in Fig. 6 is close to the k_λ reported by Liu et al ($k_\lambda = 0.15$ MPa $\sqrt{m}$ at 800°C) [24].

It is important to note that the strengths of FL ternary alloys are much higher than that of FL binary alloys with similar lamellar spacing. Considering the similar colony size of both kinds of alloys, the high strength of FL ternary alloys is most likely to be contributed by the solid solution strengthening of Nb additions. The friction stress σ_o in the Hall-Petch equation at 900 °C is 267 MPa for ternary TiAl-10Nb alloys, nearly 100 MPa higher than

that of binary TiAl alloys (178 MPa). On the other hand, the advantage of low Al content is attributed to the narrow lamellar spacing due to increasing thinner α_2 plates. Fig. 7 shows the statistic relation between the lamellar spacing and volume fraction of α_2 phase.
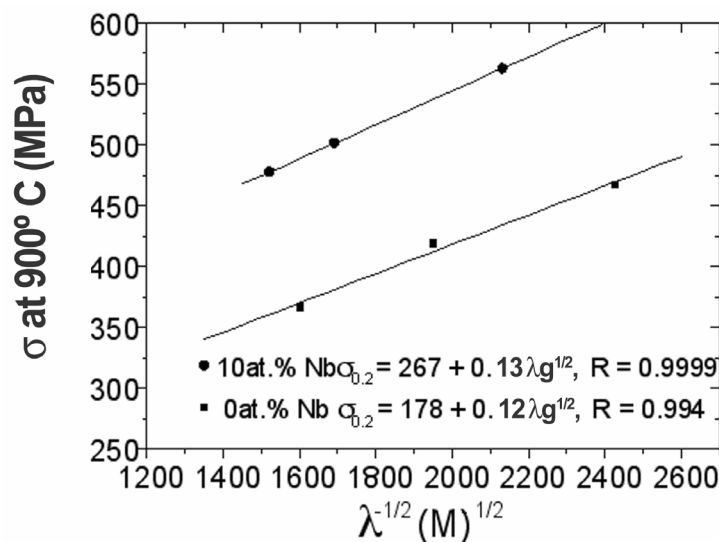

Fig.6   Hall-Petch relations for both FL binary alloys and 10 Nb containing ternary alloy with 44-49 Al contents
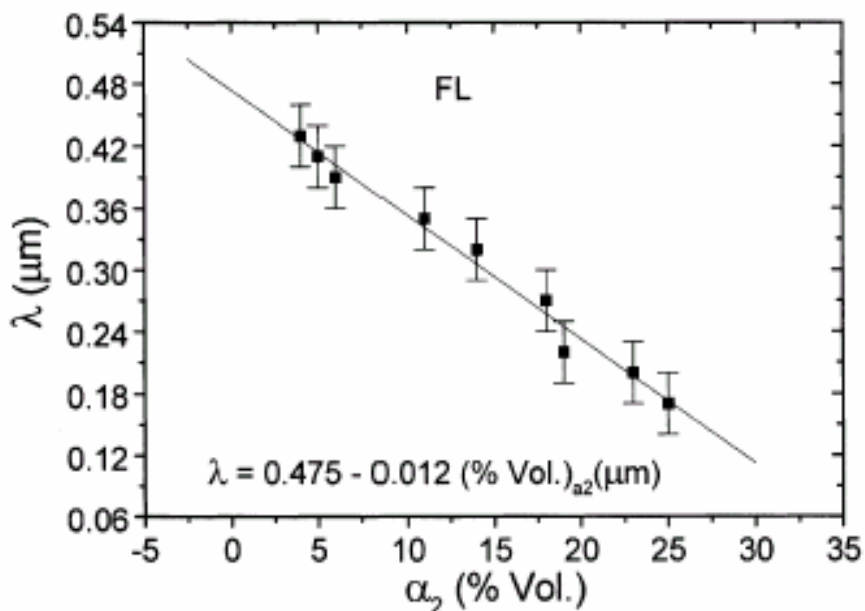

Fig. 7   Statistic relationship between lamellar spacing λ and the volume fraction of α_2 phase

Creep properties and structural changes for high temperature TiAl alloy

In section 2 it has shown that the melting point of high temperature TiAl alloys exceeds the conventional TiAl alloys by 100 °C, and high Nb may improve the microstructure stability and high temperature strength after exposure at high temperature. Fig. 8 plots the 900 °C yield strength for different alloys with FL microstructure after exposure at 1050C/30 h (DFL microstructure). The FL microstructure for high Nb alloys is much more stable, and has

significance in high temperature strength. It can be seen that the coarsening of lamellar laths during exposure significantly occurs for the binary alloy, but the microstructure degradation of the alloy with high Nb content is much slight. Particularly, the microstructure change in the grain boundary area is much more significant for the binary alloy.
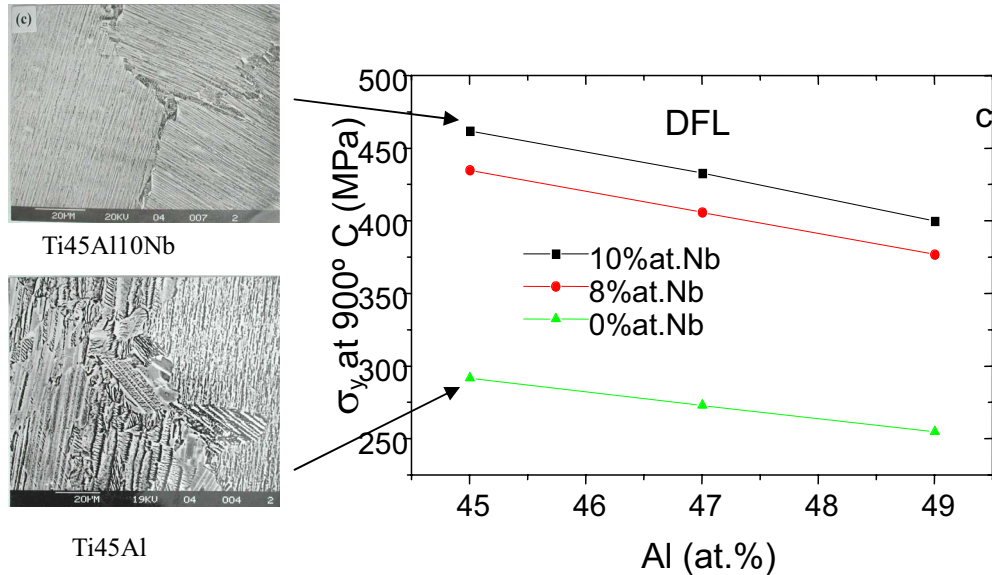

Fig. 8   Effects of high temperature exposure at 1050 °C for 30 hours on the microstructure and yield strength for binary and ternary alloys

Fig.9 shows the tensile creep curves at constant temperature of 760 °C and stresses of 142 MPa, 210 MPa and 300 MPa of high temperature TiAl alloy. The creep tests were interrupted at the times of 315, 213 and 116 hrs for the stresses of 142 MPa, 210 MPa and 300 MPa, respectively. TEM observations show the dissolution of original α_2 lamellar and new α_2 lamellar precipitation from original γ lamellar during long time creep, resulting in the increase in amount of α_2 lamellar and γ lamellar spacing.   The widening γ lamellar spacing is probably the reason why the creep rate slowly increases with creep time of second stage.

The minimum creep rate is reduced with decreasing the applied stress and the minimum creep rate at 142 MPa is very low as $1.8 \times 10^{-10} s^{-1}$, which is lower by one order of magnitude than that for K5 alloy at same test condition. The minimum creep rate at 760 °C 210 MPa for high temperature TiAl alloy decreases by two times, compared to the Ti48Al2W0.5Si alloy at same test condition. The minimum creep rate at 815 °C 138/210 MPa for K5 alloy is 2.5/2 times larger than that for high temperature TiAl at 815 °C 140/210 MPa. In sum, the minimum creep rate at 760 °C and same applied stress for high temperature TiAl alloy decreases by 2-10 times, compared to that for conventional TiAl alloy; and the minimum creep rate at 815 °C and same applied stress for high temperature TiAl alloy decreases by about 2-3 times.

Fig. 10 plots the curve of minimum creep rates of high temperature TiAl alloy. The creep data at 676-760 °C and different applied stresses for the conventional TiAl alloys are also plotted in the figure for comparison.   It notes that except two experimental points of the conventional TiAl alloys lie on the curves of the high temperature TiAl alloy all other data of minimum creep rates of conventional TiAl alloys are higher than that for high temperature TiAl alloys. The creep temperatures of these two points lied on the curve are

60-100 ^{o}C lower than that for high temperature TiAl alloy. Similarly, the creep strength of high temperature TiAl alloy is higher up to 50-150MPa.
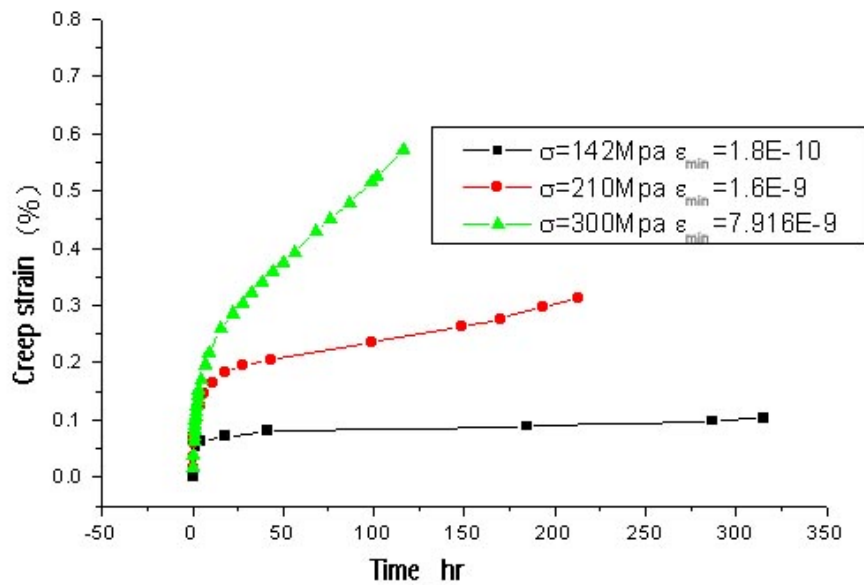

Fig. 9   Interrupted tensile creep curves at constant temperature of 760 ^{o}C and stresses of 142 MPa, 210 MPa and 300 MPa for high temperature TiAl alloy (interrupted at 315 , 213 and 116 hrs respectively)
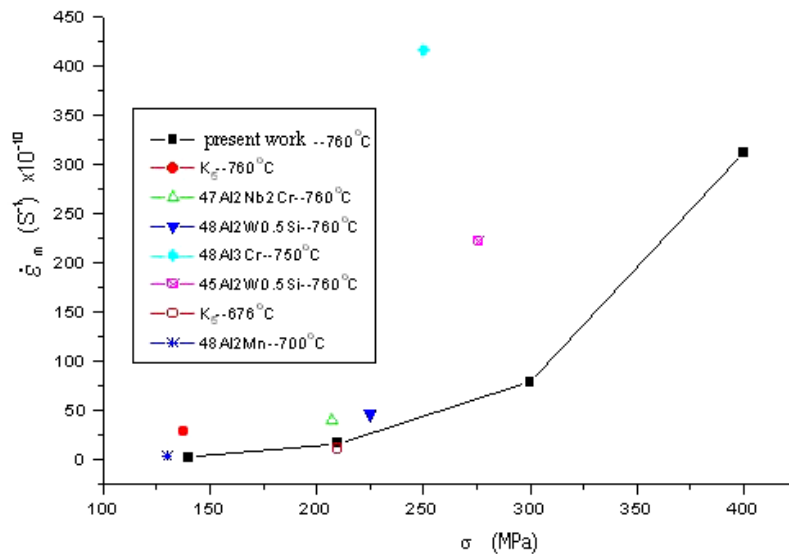

Fig. 10   Minimum creep rates of high temperature TiAl alloy and conventional TiAl alloys at 676-760 ^{o}C and different applied stresses

161

The creep mechanism for high temperature TiAl alloy is similar to conventional TiAl alloy. Creep stress exponents, the dislocation substructure and deformed microstructure near the fracture show that the creep mechanism at 760-815 ^{o}C 140-400MPa is dislocation climb of recovery creep. The higher creep strength is attributed to increasing bond and order energy, improving microstructure stability, and lowering SFE and perhaps diffusion coefficient. These effects of high Nb content in the alloy on the movement climb of dislocations have been determined to be very significant [25,26].

The influence of microstructure on the creep strength has been experimented. Fine lamellar spacing, straight lamellar boundary and zigzag colony boundary, and avoidance of GB small γ and β phase can lead to higher creep strength. Fig. 11 shows an example.
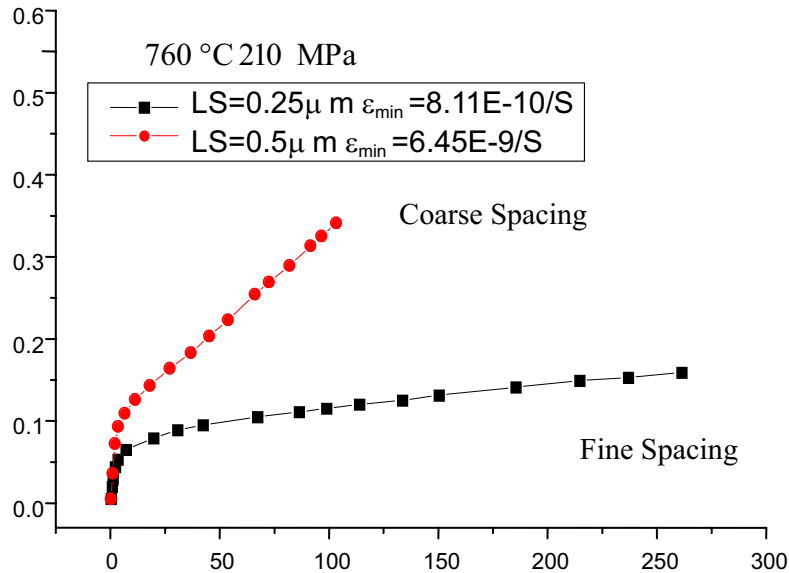

Fig. 11   Effects of lamellar spacing on the creep curves for the high temperature TiAl alloy with GS of 80μm

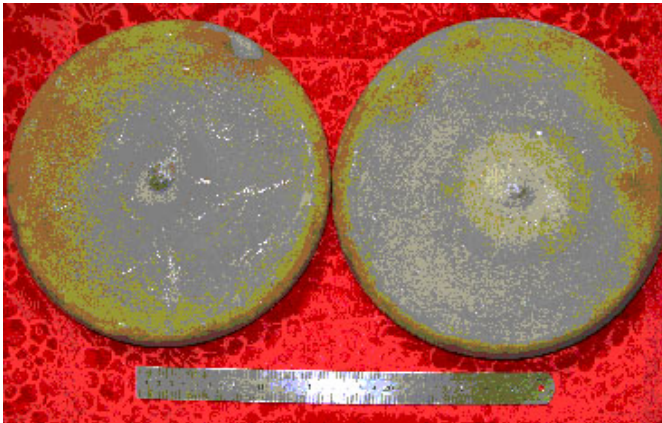**Processing and application of high temperature TiAl Alloy**

Vacuum arc re-melting (VAR), induction skull melting (ISM) and preferred plasma arc cold-hearth melting (PACHM) are used to produce a high temperature TiAl ingot from master alloying elements. Primary ingot break-down has been accomplished utilizing forging or extrusion. Fig. 12 shows plasma arc melting ingot, isothermal forging pancake, casting bar and rolling plate. The microstructure of the pancake with a duplex microstructure (DP) consists of lamellar colonies, equiaxed γ phase with the grain size of about 20-30μm and the βB2 phase at grain boundaries due to the segregation of Nb and W. The homogenous near gamma (NG) microstructure with the grain size of about 20μm and the homogeneous refined FL structure were achieved by followed heat treatments. The high temperature TiAl plate with the thickness of 2 mm was successfully fabricated on the conventional rolling mill. The overall rolling reduction is about 80%. And the surface appearance of the sheet is very good. Microstructure observation indicated that the dynamic recrystallization takes place during the high temperature rolling.
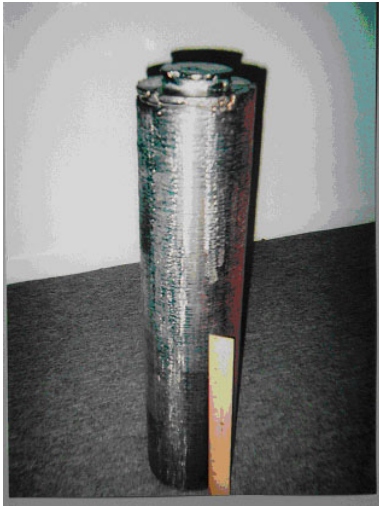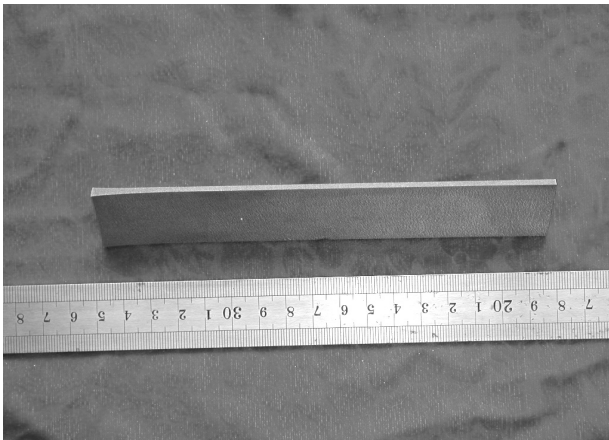
(a)   (b)

(c)

(d)

Fig. 12   Plasma melted ingot (a), casting bar (b), isothermal forging pancake (c) and plate
(d) for high temperature TiAl alloy

The main aim of the application of high temperature TiAl alloy is the substitution for high strength Ni-base superalloys for ring, disc and elevated temperature blade application. Because the density of the high Nb containing TiAl alloy is 4.3 only, nearly 50% weight saving could be achieved. The oxidation resistance of the high temperature TiAl alloy is higher than that for conventional TiAl alloys, which can be comparable to the best Ni-base superalloy Inco713C. Important physical properties of high temperature TiAl alloy are similar to conventional TiAl alloys. The RT ductility is possible problem for application, so that the forging part may be priority application. However, the RT ductility could be improved by optimization of the composition, processing and heat treatment. Now we can achieve the RT tensile elongation up to 1.5-2% in air and fracture toughness 17 MPa/m$^{1/2}$.

New development of the high Nb containing alloys for raising service temperature

A new intermetallic phase γ_1 has been found in the Ti-Al-Nb ternary system[27]. The chemical formula of the γ_1 phase was determined to be $Ti_4Nb_3Al_9$ with the density of 4.32. The unit cell of the γ_1 phase contains 16 atoms and is 4 times larger than that of the γ-TiAl phase with L1$_0$ structure. The relationship of lattice parameters between the γ and γ_1 phases is: $a_{\gamma 1} = \sqrt{2}\, a_\gamma$ and $c_{\gamma 1} = 2c_\gamma$. The x-ray diffraction pattern of stoichiometric γ_1 phase, $Ti_4Nb_3Al_9$, and the typical atom occupation in the unit cell as well as the reciprocal lattice of γ_1 phase are all determined. Nb atom in TiAl was confirmed to be substituted for Ti and preferentially occupies the Ti sublattice by the method of Atom Location Channeling Enhanced Microanalysis (ALCHEMI). For the case of low Nb content the site occupation of Nb atoms is random in the Ti sublattice. With increasing Nb content the distribution of Nb atoms in the sublattice gradually becomes ordered. The development of the Nb ordering on the Ti sublattice finally leads to the formation of a new ternary compound γ_1.

We have demonstrated the mechanical properties of the high-Nb containing γ_1-base intermetallic alloy. All γ_1 base alloys, including single phase $Ti_{3.5}Nb_{3.5}Al_9$ and multiphase $Ti_3Nb_4Al_7$, Ti20Nb60Al, Ti18Nb48Al alloys, exhibit higher compressive yield strengths in the temperature range of 20-1100 °C than high-Nb containing γ-TiAl alloy, seeing Fig. 13 [27]. In addition, the specific gravities of these multiphase alloys are low (4.7). Very high Nb content reduces the oxidation resistance of the alloys due to formation of $NbAlO_4$ or high-Nb containing oxides, but could be improved by Y addition (Fig. 14). However, the oxidation resistance of all high Nb alloys is better than that of binary TiAl alloy.
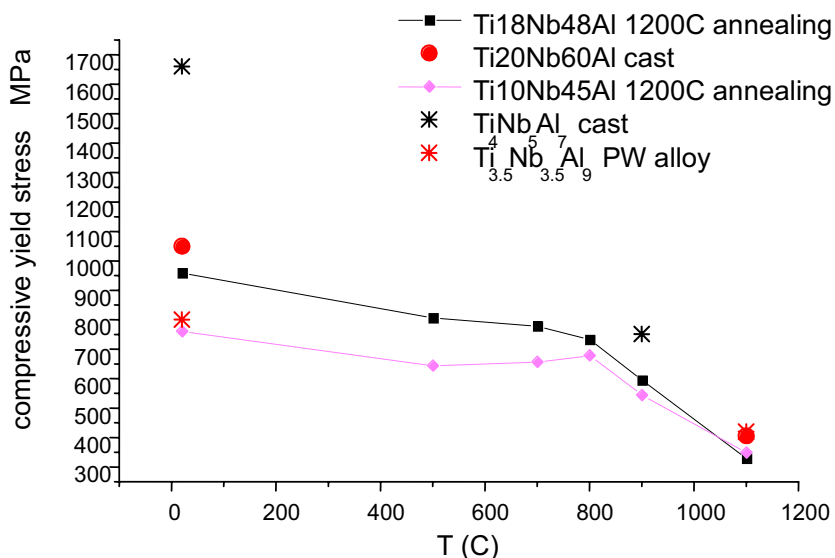
Summary

Fig. 13 Yield strengths of selected high Nb containing alloys at room and high temperature

The recent worldwide researches have interested in the development of the high temperature TiAl alloy (high Nb containing). Alloy design, processing and properties of high temperature TiAl alloy have been developed to such an extent that some structural parts can be fabricated with a balance of engineering properties. These state-of-the-art alloys have the great advantage that the service temperature is 60-100 ^{o}C higher than conventional TiAl
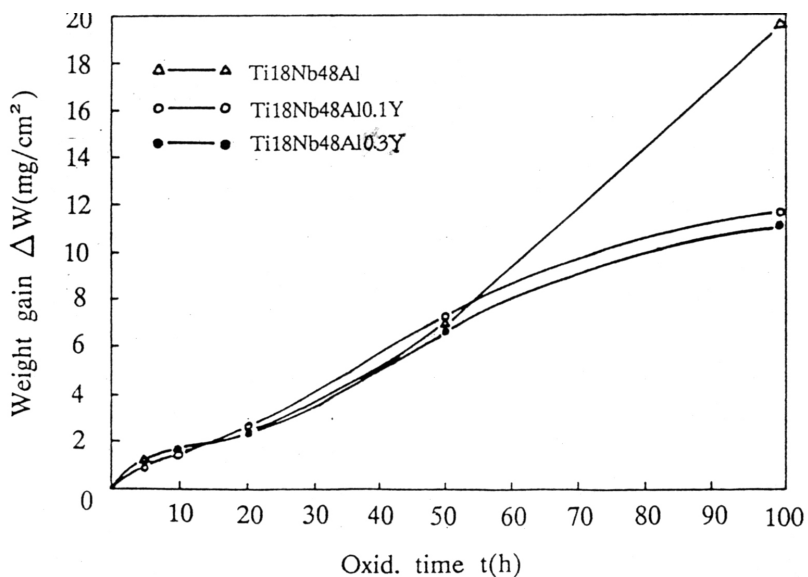

Fig. 14   Isothermal oxidation curves of Ti18Nb48Al with and without Y at 1100°C

alloy. The expected application is very attractive, but the research community faces the challenges: improving the ambient ductility, damage tolerance, fatigue resistance as well as new approach of component design.

Acknowledgement

References

1. F. Appel, R. Wagner, in Gamma Titanium Aluminides, eds. Y.W. Kim, R. Wagner a Yamaguchi etc. , TMS   Warrendale , PA , (1995) 231.
2. F. Appel, P.A. Beaven, R. Wagner, Acta Metall. Mater., 41 (1993) 1721.
3. G..L. Chen, Z.Q. Sun, and X. Zhou, Corrosion, 11(1992), 939.
4. G.L. Chen, X.T. Wang, K.Q. Ni et al., Intermetallics, 4(1996) 13
5. H. Nakamura, M. Takeyama, Y. Yamabe, M. Kikuchi, Scripta Metall. Mater., 28(1993) 997
6. G.. Chen, Z. Sun, X, Xie, Y. Ren, Y. Xu, K. Yao, X. Zhou, L. Sha, S. Fu and W. Yang, Proc. C-MRS International '90, V.2, Elsevier, Amsterdam, (1991)803.
7. G.L. Chen, Z.Q. Sun, and X. Zhou, Mater. Sci. Eng. A, 153(1992)597.
8. W.J. Zhang, G.L. Chen, and Z.Q. Sun, Scripta Metall. Mater., 28(1993)563.
9. G.. Chen., W. Zhang, Y. Wang, J. Wang and Z. Sun, Structural intermetallics, eds. R. Darolia, J.J. Lewandowski, C.T. Liu, P.L. Martin, M. V. Nathal, TMS Warrendale, PA, (1993)319.
10. G.L. Chen, J.G. Wang, L.C. Zhang, H.Q. Ye, Acta Metallurgica Sinica (English letters), 8(1995) 273.
11. G.L. Chen, L.C. Zhang, W.J. Zhang, Intermetallics, 7(1999) 1211.
12. G.L. Chen, W.J. Zhang, Z.C. Liu, S.J. Li, Y-W, Kim, Gamma Titanium Aluminizes 1999, ed .Y-W Kim, D.M. Dimiduk, N.H. Lerotto, TMS, (1999)371.
13. W.J. Zhang, S.C. Deevi, G.L. Chen, Intermetallics, 10(2002) 403.
14. Z.C. Liu, J.P. Lin, S.J. Li and G.L. Chen, Intermetallics, 10(2002) 653.
15. Y-W Kim, in Gamma Titanium Aluminides, eds. Y-W Kim, R. Wagner and M. Yamaguchi etc., TMS, Warrendale, PA, (1995)637.
16. S.-C. Huang, Structural Intermetallics, eds. R. Darolia, J.J. Lewandowski, C.T. Liu, P.L. Martin, D.B. Miracle and M.V. Nathal, TMS, Warrendale, PA, (1993) 299.
17. J.D.H. Paul, F. Appel and R. Wagner, Acta Metall., 46(1998) 1075.
18. T.T. Cheng and M.H. Lorotto, Acta Metall., 46(1998) 4801.
19. M. Yoshihara and K. Miura, Intermetallis, 3(1995) 357.
20. F. Appel, U. Lorenz, J.D.H. Paul, M. Oehring, Gamma Titanium Aluminides, eds. Y.W. Kim, D.M. Dimiduk, Loretto M. H, TMS. Warrendale, PA, (1999)381.
21. Li YG, Loretto MH. Phy Stat Sol (a), 150 (1995)271.
22. J.H. Paul, F. Appel, Aeromat 2002, (2002)79.
23. Liu Zicheng, Wang Yanli, Lin Junping, Zhang Weijun, Chen Guoliang, Trans. Nonferrous Met. Soc. China, 12(2002) 1081.
24. C. T. Liu and P. J. Maziasz, Intermetallics, 6 (1998) 653.
25. S. J. Li，Z. C. Liu, J. P. Lin, G. L. Chen, W. J. Zhang, Rare Metal Materials and Engineering, 31(2002)31.
26. X.P.Song, G.L.Chen, J. of Materials Science letters, 20(2001) 659.
27. Guoliang Chen*, Xiaodong Ni, Junpin Lin, Jinguo Wang, Weijun Zhang, Jingwen Xu, Presented at International Symposium on Gamma Titanium Aluminides: Fundamentals 132nd TMS Annual meeting & exhibition 2003 March 2-6 San Diego California.